

# Crowdsourcing reproducible seizure forecasting in human and canine epilepsy

**Benjamin H. Brinkmann,<sup>1</sup> Joost Wagenaar,<sup>2</sup> Drew Abbot,<sup>3</sup> Phillip Adkins,<sup>3</sup> Simone C. Bosshard,<sup>4</sup> Min Chen,<sup>4</sup> Quang M. Tieng,<sup>4</sup> Jialune He,<sup>5</sup> F. J. Muñoz-Almaraz,<sup>6</sup> Paloma Botella-Rocamora,<sup>6</sup> Juan Pardo,<sup>6</sup> Francisco Zamora-Martinez,<sup>6</sup> Michael Hills,<sup>7</sup> Wei Wu,<sup>8</sup> Iryna Korshunova,<sup>9</sup> Will Cukierski,<sup>10</sup> Charles Vite,<sup>11</sup> Edward E. Patterson,<sup>12</sup> Brian Litt<sup>2</sup> and Gregory A. Worrell<sup>1</sup>**

See Mormann and Andrzejak (doi:10.1093/brain/aww091) for a scientific commentary on this article.

Accurate forecasting of epileptic seizures has the potential to transform clinical epilepsy care. However, progress toward reliable seizure forecasting has been hampered by lack of open access to long duration recordings with an adequate number of seizures for investigators to rigorously compare algorithms and results. A seizure forecasting competition was conducted on kaggle.com using open access chronic ambulatory intracranial electroencephalography from five canines with naturally occurring epilepsy and two humans undergoing prolonged wide bandwidth intracranial electroencephalographic monitoring. Data were provided to participants as 10-min interictal and preictal clips, with approximately half of the 60 GB data bundle labelled (interictal/preictal) for algorithm training and half unlabelled for evaluation. The contestants developed custom algorithms and uploaded their classifications (interictal/preictal) for the unknown testing data, and a randomly selected 40% of data segments were scored and results broadcasted on a public leader board. The contest ran from August to November 2014, and 654 participants submitted 17 856 classifications of the unlabelled test data. The top performing entry scored 0.84 area under the classification curve. Following the contest, additional held-out unlabelled data clips were provided to the top 10 participants and they submitted classifications for the new unseen data. The resulting area under the classification curves were well above chance forecasting, but did show a mean  $6.54 \pm 2.45\%$  (min, max: 0.30, 20.2) decline in performance. The kaggle.com model using open access data and algorithms generated reproducible research that advanced seizure forecasting. The overall performance from multiple contestants on unseen data was better than a random predictor, and demonstrates the feasibility of seizure forecasting in canine and human epilepsy.

- 1 Mayo Systems Electrophysiology Laboratory, Departments of Neurology and Biomedical Engineering, Mayo Clinic, Rochester, MN 55905, USA
- 2 University of Pennsylvania, Penn Center for Neuroengineering and Therapeutics, Philadelphia, PA, USA
- 3 AiLive Inc, Sunnyvale, CA, USA
- 4 University of Queensland, Centre for Advanced Imaging, Queensland, Australia
- 5 Hemedics Inc, Boston, MA, USA
- 6 CEU Cardenal Herrera University, Valencia, Spain
- 7 Sydney, Australia
- 8 New York, NY, USA
- 9 Ghent University, Ghent, Belgium
- 10 Kaggle, Inc. New York NY, USA
- 11 University of Pennsylvania, School of Veterinary Medicine Philadelphia, PA, USA
- 12 University of Minnesota, Veterinary Medical Center, St. Paul, MN, USA

Received September 29, 2015. Revised December 09, 2015. Accepted January 28, 2016. Advance Access publication March 31, 2016

© The Author (2016). Published by Oxford University Press on behalf of the Guarantors of Brain.

This is an Open Access article distributed under the terms of the Creative Commons Attribution Non-Commercial License (<http://creativecommons.org/licenses/by-nc/4.0/>), which permits non-commercial re-use, distribution, and reproduction in any medium, provided the original work is properly cited. For commercial re-use, please contact [journals.permissions@oup.com](mailto:journals.permissions@oup.com)

Correspondence to: Benjamin H. Brinkmann, PhD,  
Department of Neurology,  
Mayo Clinic, 200 First Street SW,  
Rochester, MN 55905, USA  
E-mail: Brinkmann.Benjamin@mayo.edu

**Keywords:** epilepsy; intracranial EEG; refractory epilepsy; experimental models

**Abbreviations:** AUC = area under the curve; FFT = fast Fourier transform; iEEG = intracranial electroencephalography; SVM = support vector machine

## Introduction

The apparently random nature of seizures is a significant factor affecting the quality of life for patients with epilepsy (Fisher, 2000; Schulze-Bonhage and Kuhn, 2008). Despite taking daily medications many patients with epilepsy continue to have seizures (Kwan *et al.*, 2010; Kwan and Brodie, 2010). Accurate seizure forecasting could transform epilepsy care, allowing patients to modify activities to avoid risk and take antiepileptic drugs only when needed to stop seizures before they develop. However, to achieve clinically relevant seizure forecasting, better methods are needed for identifying periods when seizures are likely to occur (Cook *et al.*, 2013). Significant evidence has emerged supporting the idea that seizures arise from an identifiable preictal brain state (Stacey *et al.*, 2011; Cook *et al.*, 2013). Clinical studies describe patients self-reporting seizure-prone states prior to seizure at a rate greater than chance (Haut *et al.*, 2007), and changes in cerebral blood flow, oxygenation, and cortical excitability have been reported prior to seizures (Baumgartner *et al.*, 1998; Adelson *et al.*, 1999; Aarabi *et al.*, 2008; Badawy *et al.*, 2009).

While many early seizure forecasting studies using EEG features suffered from inadequate statistical analysis, particularly with regards to adequate sampling of the interictal period (Mormann *et al.*, 2007; Andrzejak *et al.*, 2009), recent studies have demonstrated in a rigorous statistical framework (Snyder *et al.*, 2008) that human and canine seizure forecasting is possible (Cook *et al.*, 2013; Howbert *et al.*, 2014; Teixeira *et al.*, 2014; Brinkmann *et al.*, 2015). A major challenge for seizure forecasting research has been the lack of long duration recordings with adequate interictal data and number of seizures for rigorous statistical testing (Mormann *et al.*, 2007; Andrzejak *et al.*, 2009). The majority of early studies were limited to relatively short human intracranial EEG (iEEG) recordings obtained as part of epilepsy surgery evaluations. These clinical iEEG studies from the epilepsy monitoring units rarely extend beyond 10 days and are enriched with seizures because the antiepileptic drugs are tapered to expedite the evaluation (Duncan *et al.*, 1989). These clinical records rarely yield an adequate number of seizures separated by clear interictal periods for rigorous statistical testing, and thus are limited in their usefulness to develop predictors of patients' habitual seizures (Marciani *et al.*, 1985; Duncan *et*

*al.*, 1989). Longer-duration iEEG recordings have been analysed from epileptic animal models where an artificial epileptic focus is created (Bower and Buckmaster, 2008; Fujita *et al.*, 2014), but the usefulness of these models to develop algorithms for forecasting naturally occurring focal epilepsy remains unclear (Loscher, 2011).

Recent studies have applied machine learning techniques to seizure forecasting with promising results (Mirowski *et al.*, 2009; Park *et al.*, 2011; Howbert *et al.*, 2014). While many apply rigorous statistics to their results (Snyder *et al.*, 2008), the scarcity of long duration recordings with adequate seizures remains an obstacle, as does the inability to directly compare algorithm performance from different research groups using common data. Recently an implantable seizure advisory system developed by NeuroVista Inc. made possible wireless telemetry of 16 channels of iEEG (sampling at 400 Hz) to a patient advisory device capable of running a real-time seizure forecasting algorithm (Davis *et al.*, 2011; Cook *et al.*, 2013). Initially the device was validated in canines with naturally-occurring epilepsy (Davis *et al.*, 2011; Coles *et al.*, 2013; Howbert *et al.*, 2014). Naturally-occurring canine epilepsy is an excellent platform for human epilepsy device development (Leppik *et al.*, 2011; Patterson, 2014) as dogs can be large enough to accommodate human devices, and their epilepsy is similar clinically (Potschka *et al.*, 2013; Packer *et al.*, 2014) and neurophysiologically (Berendt *et al.*, 1999; Berendt and Dam, 2003; Pellegrino and Sica, 2004) to human epilepsy. Canine epilepsy is treated with many of the same medications at dosages comparable to human epilepsy (Farnbach, 1984; Dowling, 1994), and canine epilepsy is refractory to these medications at a comparable rate to human epilepsy (Govendir *et al.*, 2005; Munana *et al.*, 2012; Kiviranta *et al.*, 2013). In a recent landmark clinical pilot study, NeuroVista and a team of Australian researchers implanted this device in 15 patients with drug-resistant epilepsy (<http://ClinicalTrials.gov>, study NCT01043406), and achieved seizure forecasting sensitivity of 65–100% in 11 patients during algorithm training, and eight patients prospectively after 4 months. In addition, the seizure advisory system was able to forecast low seizure likelihood periods with >98% negative predictive value in five patients tested (Cook *et al.*, 2013).

Despite these advances, improvements are needed in sensitivity and specificity of seizure forecasting algorithms to

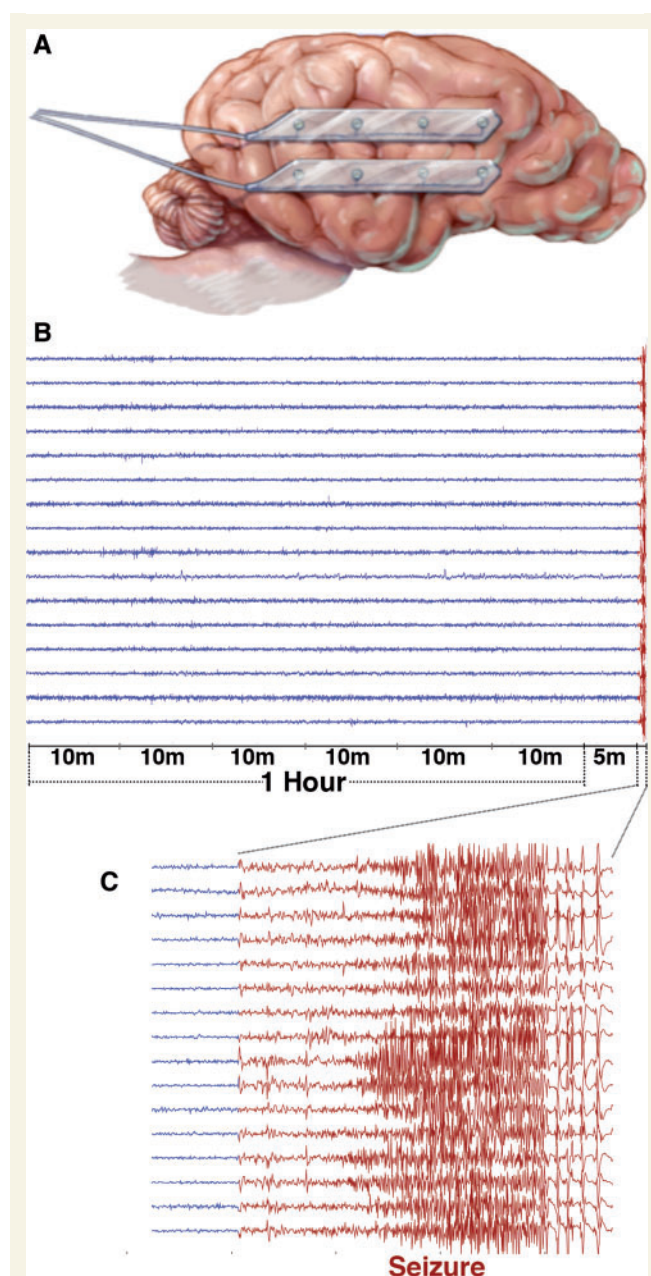


**Figure 1** Canine electrode locations and data segments.

(A) For the canine subjects, bilateral pairs of 4-contact strips were implanted oriented along the anterior-posterior direction. Electrode wires were tunneled through the neck and connected to an implanted telemetry device secured beneath the latissimus dorsi muscle. (B) An hour of data with a 5-min offset before each lead seizure was extracted and split into 10-min segments for analysis. (C) The expanded view illustrates a ~35-s long seizure.

attain clinically useful performance, and publicly available chronic iEEG datasets are needed to directly compare algorithms in a model relevant to human epilepsy. To stimulate reproducible research and improve the state of the art in seizure forecasting algorithms, the American Epilepsy Society, Epilepsy Foundation of America, and National Institutes of Health sponsored an open invitation competition on kaggle.com in 2014 using iEEG data from canines

and humans with epilepsy. Contestants were provided with labelled interictal and preictal iEEG training data, and unlabelled testing iEEG data from ambulatory recordings taken with the NeuroVista seizure advisory system device in five canines with naturally occurring epilepsy, and wide bandwidth (5 kHz) presurgical iEEG recordings from two patients with epilepsy. The contestants used a wide range of supervised machine learning algorithms of their choice that were trained on available labelled training data and attempted to accurately label the unknown ‘testing data’ clips as preictal or interictal. Following the competition, the top performing algorithms were further tested on held-out, unseen data clips to assess the generalizability and robustness of algorithms developed via the kaggle.com forum.

## Materials and methods

### Subjects and data

Intracranial EEG data were recorded chronically from eight canines with naturally occurring epilepsy using the NeuroVista seizure advisory system implanted device described previously (Davis *et al.*, 2011; Coles *et al.*, 2013). The dogs were housed at the veterinary hospitals at the University of Minnesota and University of Pennsylvania. Sixteen subdural electrodes were implanted intracranially in each canine in a bilaterally symmetrical arrangement (Fig. 1), with paired four-contact strips oriented from anterior to posterior on each hemisphere. The electrode wires were tunneled caudally through openings in the cranium, anchored, looped and passed under the skin to the implanted telemetry unit medial to the dog’s shoulder. Wires were connected to a recording device, which was implanted under the latissimus dorsi muscle and iEEG data were wirelessly telemetered to a receiver and storage unit in a vest worn by the dog. Recorded data were stored on removable flash media, which were periodically removed and copied via the internet to a cloud storage platform for subsequent analysis. The implanted recording device was powered by a rechargeable battery unit, which was charged daily by monitoring personnel. Recorded iEEG from the 16 electrode contacts was referenced to the group average. Of the eight implanted canines, five produced high quality iEEG data and had an adequate number of seizures recorded for analysis. Two of the eight dogs had no seizures, and one dog had two seizures following implantation surgery.

Epilepsy patients who underwent wide bandwidth (5 kHz sampling) iEEG monitoring for drug-resistant epilepsy at Mayo Clinic Rochester were reviewed. Subjects with poor data quality or other technical issues were excluded from further analysis, as were patients with fewer than four recorded lead seizures, defined as seizures occurring without a preceding seizure for a minimum of 4 h. Two patients were chosen with long recordings of high quality iEEG data and maximum possible separation between lead seizures. The patients’ electrode configurations and placement had been determined by clinical considerations, and are illustrated in Fig. 2. Patient 1 was a 70-year-old female with intractable epilepsy who underwent intracranial monitoring with 8-contact depth electrodes



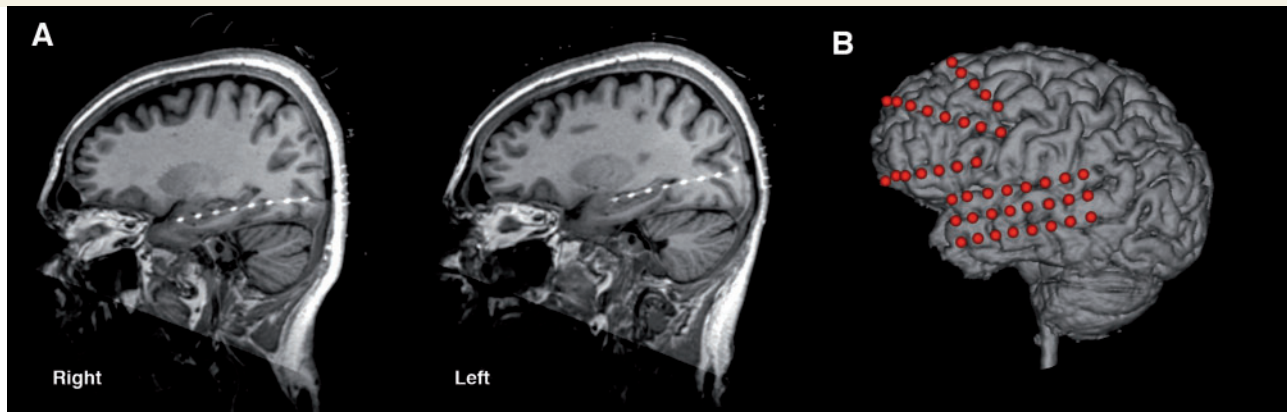


**Figure 2 Human implanted electrode locations.** Implanted electrodes are visible in X-ray CT images coregistered to the space of the patient's MRI for the two epilepsy patients whose data was used in this competition. **(A)** Patient 1 had bitemporal 8-contact penetrating depth electrodes implanted along the axes of the left and right hippocampus. **(B)** Patient 2 had a  $3 \times 8$  subdural electrode grid placed along the axis of the left temporal lobe and frontal lobe strip electrodes. Spheres represent approximate electrode positions due to post-craniotomy brain surface shift in the CT. Electrodes not used in these experiments have been omitted from this illustration.

placed from a posterior approach in each temporal lobe and into the hippocampus. There were 71.3 h of iEEG data with five annotated seizures, four of which were lead seizures. Patient 2 was a 48-year-old female with intractable epilepsy who had a  $3 \times 8$ -contact subdural electrode grid placed over her left temporal lobe in addition to two 4-contact depth electrodes in each of the right and left temporal lobes, two left subtemporal 4-contact strip electrodes, and three left frontal 8-contact strips. This patient was monitored for 158.5 h recording 41 seizures, six of which met criteria for lead seizures. To limit data size, only data from the  $3 \times 8$  subdural grid were used in the competition, as this grid covered both seizure onset zone and non-pathological tissue. These research iEEG data were acquired in parallel with the patient's clinical recording as described previously (Brinkmann *et al.*, 2009).

All iEEG data records were reviewed and seizures annotated by a board certified epileptologist (G.A.W.). Preictal data clips were extracted from the 66 min prior to lead seizures in six 10-min data clips. The preictal data clips were spaced 10 s apart in time, and offset by 5 min prior to the marked seizure onset to prevent subtle early ictal activity from contaminating the final preictal data clip. Interictal clips were selected similarly in groups of six 10-min clips with 10-s spacing beginning from randomly selected times a minimum of 1 week from any seizure. Each extracted data segment was individually mean centred. Data segments were stored as ordered structures including sample data, data segment length, iEEG sampling frequency, and channel names in uncompressed MATLAB format data files. Training data files also included a sequence number indicating the clip's sequential position in the series of six 10-min data clips. The temporal sequence of the training and testing data was not made available to the contestants. The full data record was divided approximately in half, with labelled training interictal and preictal data clips taken from the first portion and unlabelled testing data clips from the last portion of the record. The division of testing and training data was selected to make an adequate number of lead seizures available for both training and testing (Table 1). Data clips for each subject were stored in separate folders and bundled

into separate zip-compressed file archives which ranged between 2.6 GB and 14.83 GB. The total size of the data for the seven subjects was 59.64 GB. Compressed file archives were linked on the contest page at kaggle.com (<https://www.kaggle.com/c/seizure-prediction/data>) and made available for download by contestants. All data remain available for download at [ieeg.org](http://ieeg.org) and [msel.mayo.edu/data.html](http://msel.mayo.edu/data.html).

The contest ran from 25 August to 17 November 2014. Contestants were permitted to develop algorithms in any computer language and using any features, classification and data processing methods they chose, but classifications were required to come directly from an algorithm—classification by visual review was prohibited. Algorithms were also required to use a uniform data processing method for all subjects, but were permitted to modify data processing methods based on data parameters, such as sampling frequency. Contestants uploaded preictal probability scores (a floating point number between 0 and 1 indicating the probability of each clip being preictal) for the 3935 testing data clips in a comma separated values file, and a real-time public leader board on kaggle.com provided immediate feedback on classification accuracy. Public leader board scores were computed on a randomly sampled 40% subset of the test data clips, but official winners were determined based on the remaining 60% of the testing data (Fig. 3). Classification scores were computed by Kaggle as the area under the receiver operating characteristic (ROC) curve created by applying varying threshold values to the probability scores. Contestants were permitted five submissions per day at the beginning of the contest, and 10 submissions per day for the final 2 weeks. Prizes were awarded for first (\$15 000), second (\$7000), and third (\$3000) place finishers as determined by the private leader board scores. Winning teams were required to submit their algorithms under an open source license to be made publicly available on via the IEEG portal ([ieeg.org](http://ieeg.org)) and the Mayo Systems Electrophysiology Lab (MSEL.mayo.edu/data.html).

Following the competition, the top 10 finishing teams were invited to run their algorithms on a held-out set of unseen data clips to assess the robustness of the algorithms developed on

**Table 1** Data characteristics for the Kaggle.com seizure forecasting contest and held-out data experiment

Subject	Sampling rate (Hz)	Recorded data (h)	Seizures	Lead seizures	Training clips (% interictal)	Testing clips (% interictal)	Held-out clips (% interictal)
Dog 1	400	1920	22	8	504 (95.2)	502 (95.2)	2000 (99.7)
Dog 2	400	8208	47	40	542 (92.3)	1000 (91.0)	1000 (100)
Dog 3	400	5112	104	18	1512 (95.2)	907 (95.4)	1000 (100)
Dog 4	400	7152	29	27	901 (89.2)	990 (94.2)	1000 (95.8)
Dog 5	400	5616	19	8	480 (93.8)	191 (93.7)	0
Patient 1	5000	71.3	5	4	68 (73.5)	195 (93.9)	0
Patient 2	5000	158.5	41	6	60 (70.0)	150 (90.7)	0

new data. An additional 5000 unlabelled data clips from four of the five original dogs (Table 1) were provided to these contestants. These clips were from the same data records but represented new, unseen, iEEG data from the original dataset. For this dataset a higher proportion of interictal to interictal data (100:1) was selected in an attempt to more closely approximate the preictal:interictal ratio in patients having a few seizures per month. Participants again submitted probability scores for the holdout data in a comma separated values format, and results were scored as the area under the ROC curve. Participants who used aggregations of multiple machine learning techniques also submitted separate classifications for each technique. Six of the top 10 teams (Table 2), including the three winners, agreed to participate in the holdout data experiment and provide detailed descriptions of their algorithms. The team with the top overall score, area under the curve (AUC) = 0.84, chose to forfeit the prize to avoid disclosing source code and pursue an algorithm patent. This team did not participate in the subsequent analysis of held-out data.

Data used in this competition as well as the source code for the top performing algorithms are freely available on the International IEEG Portal (<http://ieeg.org>), and the Mayo Systems Electrophysiology Lab ftp site (<http://msel.mayo.edu/data.html>).

## Algorithms

Algorithms are described below and summarized in Table 3 in order of performance on the private leader board. More detailed information regarding the top finishers' algorithms can be found in the Supplementary material.

### First place team

The first place team's approach consisted of an ensemble of three distinct algorithms:

#### Algorithm 1

Intracranial EEG data were sampled in sequential 1-min windows, in which were calculated spectral entropy and Shannon's entropy (MacKay, 2003) at six frequency bands: delta (0.1–4 Hz), theta (4–8 Hz), alpha (8–12 Hz), beta (12–30 Hz), low-gamma (30–70 Hz) and high gamma (70–180 Hz), and Shannon's entropy in dyadic (between 0.00167 and 109 Hz spaced by factors of  $2^n$ ) frequency bands. The feature set also included the spectral edge at 50% power below 40 Hz, spectral correlation between channels in dyadic frequency bands, the time series correlation matrix and its

eigenvalues, fractal dimensions, Hjorth activity, mobility and complexity parameters (Hjorth, 1970), and the statistical skewness and kurtosis of the distribution of time series values. These features were used to train a LassoGLM classifier implemented in MATLAB (MathWorks Inc, Natick MA).

#### Algorithm 2

The iEEG data were analysed in 8-s windows with 7.75 s of overlap. Sums of fast Fourier Transform (FFT) power over bands spanning the fundamental frequency of the FFT, 1 Hz, 4 Hz, 8 Hz, 16 Hz, 32 Hz, 64 Hz, 128 Hz and Nyquist, yielding nine bands per channel, time series correlation matrix, and time series variance were computed for the feature set. A support vector machine (SVM) model (Vapnik and Vapnik, 1998) with a linear kernel was trained with bootstrap aggregation (Breiman, 1996) training on 10% of the data, and a kernel principal component analysis (PCA) (Hotelling, 1933) decomposition of the features was performed with basis truncation. The algorithm was implemented in python using the scikit-learn toolkit (<http://scikit-learn.org/stable/modules/svm.html>).

#### Algorithm 3

This algorithm used the same 8-s overlapping iEEG windows and features as Algorithm 2 above. Classification was accomplished using a random forest algorithm with 80 trees implemented in MATLAB. For this model adjacent window scores were interpolated by a factor of 8 using a cubic spline algorithm before ensembling.

The three numerical models were median centred and an ensemble of the three models was created using an empirically determined weighted average: ( $1/4 \times \text{Random Forest} + 1/4 \times \text{Bagged SVM} + 1/2 \times \text{LassoGLM}$ ). In the held-out data experiment this team submitted classifications produced separately by each of these algorithms to assess their relative contributions, as well as the final ensemble result.

### Second place team

The second place algorithm downsampled the iEEG data to 100 Hz and analysed the data in 50-s non-overlapping windows. The set of iEEG-derived features consisted of the logarithm of the FFT magnitude in 18 equal frequency bands between 1 and 50 Hz, the inter-channel covariance and eigenvalues of these frequency bands, and the interchannel covariance and eigenvalues in the time domain. A SVM machine learning algorithm with a radial basis function (RBF) kernel ( $C = 10^{-6}$ ,  $\gamma = 0.01$ ) was trained and used to classify the power-in-band features in each analysis window. A

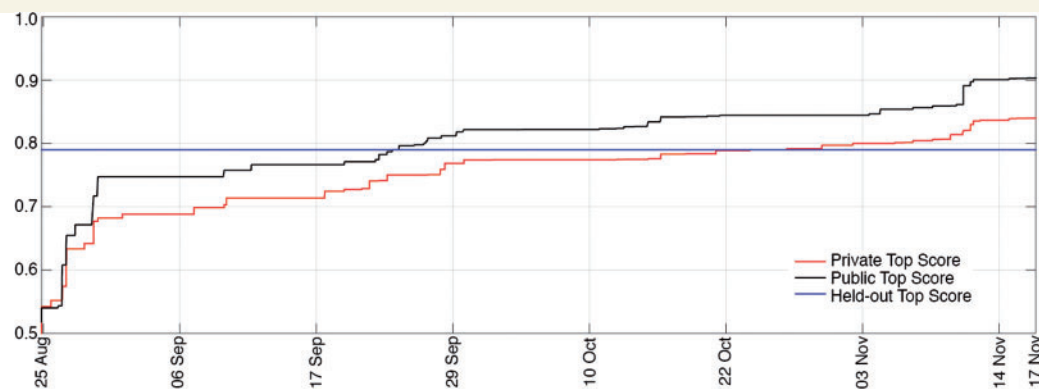


**Figure 3** Leading scores during the competition. Plots of the leading score on the kaggle.com public (black line) and private (red line) leader boards for the duration of the competition. The top score from the held-out data experiment is represented by the horizontal blue line.

**Table 2** AUC scores for top ten Kaggle.com finalists in the public and private leaderboards

Place	Team name	Public leader board	Private leader board	Entries
1	QMSDP	0.86	0.82	501
2	Birchwood	0.84	0.80	160
3	ESAI CEU-UCH	0.82	0.79	182
4	Michael Hills	0.86	0.79	427
5	KPZZ	0.82	0.79	196
6	Carlos Fernandez	0.84	0.79	299
7	Isaac	0.84	0.79	253
8	Wei Wu	0.82	0.79	140
9	Golondrina	0.82	0.78	171
10	Sky Kerzner	0.84	0.78	97

The public leader board score was computed on a randomly-chosen 40% subset of the data, while the private leader board was computed on the remaining 60%.

combination of the arithmetic and harmonic means of individual analysis windows with Platt scaling (Platt, 1999) was used to aggregate analysis windows into a single probability score for each segment. Algorithms were coded in python using the scikit-learn toolkit.

### Third place team

The third place team analysed the iEEG data in 60-s windows with 30 s of overlap. A Hamming window was applied to the data segments, and the FFT was divided into six frequency bands: delta (0.1–4 Hz), theta (4–8 Hz), alpha (8–12 Hz), beta (12–30 Hz), low gamma (30–70 Hz) and high gamma (70–180 Hz). PCA (Hotelling, 1933) and independent component analysis (ICA) (Kruskal, 1969) were applied to the six frequency bands across the sequence of 60-s windows. Eigenvalues of the frequency domain interchannel correlation matrix were computed from the original iEEG signal and the derivative of the iEEG signal over the full 10-min segment length. A Bayesian model combination of artificial neural networks with different depths and a k-nearest neighbour ( $k = 40$ ) classification algorithm was used to provide the final classification of each segment. Algorithms were coded in R (<http://www.R-project.org>) and used the APRIL-ANN machine learning toolkit (<https://github.com/pakozm/april-ann>).

[www.R-project.org](http://www.R-project.org)) and used the APRIL-ANN machine learning toolkit (<https://github.com/pakozm/april-ann>).

### Fourth place team

The fourth place team used non-overlapping 75-s windows, and the feature set included the upper right triangle (non-redundant coefficients) of the time domain correlation matrix with sorted eigenvalues, the upper right triangle of the frequency domain correlation matrix with sorted eigenvalues, the FFT magnitude with logarithmic scaling for frequency bands up to 48 Hz (0.5, 2.25, 4, 5.5, 7, 9.5, 12, 21, 30, 39, and 48 Hz), spectral entropies up to 24 Hz, as well as the Higuchi fractal dimension (Higuchi, 1988), Petrosian fractal dimension (Petrosian, 1995), and Hurst exponent (Feder, 1988). A genetic algorithm (population 30, 10 generations) was used to select features within the Petrosian fractal dimension features, the Hurst exponent features, and the Higuchi fractal dimension and spectral entropy features, using a 3-fold cross validation in the training data. A SVM with RBF kernel ( $\gamma = 0.0079$ ,  $C = 2.7$ ) was used to classify the data segments.

### Fifth, sixth and seventh place teams

The fifth, sixth, and seventh place teams did not participate in the held-out data experiment and did not provide additional detail about their algorithms.

### Eighth place team

The eighth place team downsampled the data to 200 Hz and analysed each 10-min data clip in non-overlapping 1-min windows. In each window the mean, maximum, and standard deviation in both the time and frequency domains were calculated for each channel, and for the average of all channels. The frequency with maximum amplitude in the FFT was identified for each individual channel as well. The interchannel covariance matrices were calculated in the time and frequency domains, and the mean, three highest covariances, and standard deviation were added to the set of features. The lower 20% (up to 40 Hz for the dogs and 500 Hz for the humans) of the frequency spectrum below the Nyquist limit of each channel was divided into 24 equally spaced frequency bands, and the average spectral power in each bands was included as well. The GLMNet (Friedman *et al.*, 2010) classifier (<http://cran.r-project.org/web/packages/glmnet/index.html>) was used to classify the data segments.

project.org/web/packages/glmnet/index.html) and a SVM (RBF kernel,  $C = 100$ ,  $\gamma = 0.001$ ) were trained globally across all training data, as well as separately on individual subjects using all features with a 2-fold cross validation with 10 shuffles. The classifiers were ensembled by ranking data clip probabilities from each model and computing a weighted average of all the ranks. The mean of the 1-min data windows was taken as the probability for each 10 min data clip. This algorithm was implemented in R.

### Ninth place team

The ninth place algorithm partitioned the raw iEEG data clips into non-overlapping 1-min windows. The standard deviation and average spectral power in delta (0.1–4 Hz), theta (4–8 Hz), alpha (8–12 Hz), beta (12–30 Hz), low gamma (30–70 Hz) and high gamma (70–180 Hz) frequency bands (Howbert *et al.*, 2014) were computed for each channel. A convolutional neural network (CNN) (LeCun *et al.*, 1998) was used for classification, with convolutions done in the time domain. The neural network consisted of two convolutional layers followed by a temporal global pooling layer, a fully-connected layer, and a logistic regression layer. During algorithm training, additional data windows were generated by resampling data to span consecutive data clips. The final clip probability was determined by the average of the scores generated by 11 CNNs with variations in analysis window sizes, frequency bands, and CNN architecture.

### Tenth place team

The 10th place team did not participate in the held-out data experiment.

## Results

Public and private leader board results from the competition are plotted in Fig. 2, for the duration of the contest. In total 505 teams comprising 654 individuals entered the competition and submitted classifications. A total of 17 856 classifications of the test data were submitted. Statistics for the top scoring teams are listed in Table 2. For teams participating in the held-out data experiment, the mean (max–min) public leader board score was 0.84 (0.86–0.82), private leader board score was 0.79 (0.82–0.78), and contestants made a mean (max–min) of 242.6 (501–140) entries. The mean (max–min) AUC score on the held-out data was 0.74 (0.79–0.59), representing a mean 6.85% (standard deviation 2.45%) decline relative to the mean private leader board score. AUC scores and algorithm sensitivity at 75% specificity are reported in Table 3. Full ROC curves for the contest algorithms on the held-out data are included in the Supplementary material.

## Discussion

Formulating the seizure forecasting problem as a contest on kaggle.com proved a unique way to engage a large pool of data scientists worldwide on an important problem. The opportunity for a group of independent data scientists to

analyse a large, freely available dataset from humans and canines with epilepsy yielded reproducible and directly comparable results from a range of seizure forecasting approaches. There is now widespread recognition that many published claims in biomedical research are not reproducible. (Ioannidis, 2005; Landis *et al.*, 2012; Button *et al.*, 2013) The consequences of the lack of reproducibility are profound, and inefficient use of limited resources may slow the development of therapies for patients. In the computational science and engineering communities in particular, reproducible research requires open source data and algorithms (Buckheit and Donoho, 1995; Donoho, 2010) in addition to published methods and results. Early studies in seizure forecasting were limited by both inadequate datasets and flawed statistical testing (Mormann *et al.*, 2007; Andrzejak *et al.*, 2009), and lack of openly available data and algorithms hindered investigators from challenging these results. Making the data and algorithm source code from the present study freely available (<http://ieeg.org> and <http://msel.mayo.edu/data.html>), facilitates reproducibility and provides a benchmark for future algorithm development.

This study demonstrates that seizures are not random events and supports the feasibility of real-time seizure forecasting. All six algorithms in the held-out data experiment achieved performance greater than a random chance predictor ( $P < 0.0001$ ,  $z$ -score computed relative to AUC of 0.5), as was the top scoring algorithm on the private leader board ( $P < 0.0001$ ). On the private leader board 359 teams scored above the upper 95% confidence limit AUC relative to a random classifier (0.531, Hanley-McNeil method). While no published study yet has used this full data set as a benchmark, the results compare favourably to a recent study (0.72 AUC) computing on the full continuous data from the five canines (Brinkmann *et al.*, 2015).

At a time when skills in analytics and machine learning command a high premium in the marketplace and research labs face reduced funding, an online competition can represent a cost-effective method of achieving progress on difficult problems. Access to contestants with different backgrounds and approaches can quickly and efficiently evaluate a broad range of features and algorithms. There are, however, some limitations to the online kaggle.com competition format that should be noted. First, the ability to submit multiple trials may contribute to overtraining on the contest dataset. While determining winners by the private leader board score computed on the majority of data reduces this risk somewhat, it is critical in this type of forum to provide as broad a sampling of data as possible to ensure extensibility of solutions to the real-world problem. Here this issue was further mitigated by running a post-contest analysis using withheld data not seen during algorithm development. The fact that there was a modest decline in forecasting performance suggests overtraining was not a significant factor.

Second, the necessity of providing contestants with the full set of testing data in an unlabelled form provides both an advantage and a disadvantage to contestants.



**Table 3** AUC scores for the held-out data experiment compared to scores on the public and private leader boards

Team name	Window (overlap)	Features	Machine learning algorithm	Ensemble method	Public leader board	Private leader board	Held-out data	Per cent change	Sensitivity at 75% specificity
QMSDP	60 s (0%), 8 s (97%)	Spectral power, spectral entropy, correlation, fractal dimensions, Hjorth parameters, distribution statistics, signal variance	LassoGLM, Bagged SVM, Random Forest	Weighted average	0.86	0.82	0.75	−7.97	0.71
<b>QMSDP</b>	<b>60 s (0%)</b>	<b>Spectral entropy, correlation, fractal dimensions, Hjorth parameters, distribution statistics</b>	<b>LassoGLM</b>		<b>0.84</b>	<b>0.81</b>	<b>0.73</b>	<b>−9.26</b>	<b>0.69</b>
<b>QMSDP</b>	<b>8 s (97%)</b>	<b>Spectral power, correlation, signal variance</b>	<b>Bagged SVM</b>		<b>0.79</b>	<b>0.76</b>	<b>0.76</b>	<b>0.91</b>	<b>0.73</b>
<b>QMSDP</b>	<b>8 s (97%)</b>	<b>Spectral power, correlation, signal variance</b>	<b>Random Forest</b>		<b>0.79</b>	<b>0.72</b>	<b>0.59</b>	<b>−17.88</b>	<b>0.33</b>
Birchwood	50 s (0%)	Log spectral power, covariance	SVM	Platt scaling	0.84	0.80	0.74	−8.01	0.60
ESAI CEU-UCH	60 s (50%)	Spectral power, correlation, signal derivativePCA and ICA preprocessing	Neural Network and K Nearest Neighbour clustering	Bayesian combination	0.82	0.79	0.72	−9.77	0.54
Michael Hills		Spectral power, correlation, spectral entropy, fractal dimensions, Hurst exponent Genetic algorithm feature selection	SVM		0.86	0.79	0.79	−0.29	0.73
Wei Wu	60 s (0%)	Spectral power, statistical measures, covariance matrices	SVM and GLMNet	Weighted average of rank scores	0.82	0.79	0.77	−1.86	0.69
Golondrina	60 s (0%)	Spectral power, signal standard deviation	Convolutional neural networks (test data calibration)		0.82	0.78	0.76	−2.77	0.73
<b>Golondrina</b>	<b>60 s (0%)</b>	<b>Spectral power, signal standard deviation</b>	<b>Convolutional neural networks (not calibrated on test data)</b>		<b>0.81</b>	<b>0.78</b>	<b>0.77</b>	<b>−1.39</b>	<b>0.75</b>

Rows in bold represent algorithm variations submitted after the competition as part of the held-out data experiment. Additional information on algorithms is available in the Supplementary material.



Having the testing set available gave contestants the opportunity to directly measure the full statistical range of future data, aiding normalization of models in a way not possible in prospective real-time seizure forecasting. In contrast, timing information about the testing clips could not be provided in this format, which prevented contestants from deploying background normalization strategies commonly used in time series analysis. A third limitation of the competition format is that algorithms and source code are not required to be fast, modular, or well documented, and significant development effort may be required to make even the best competition algorithm suitable for application on a broader range of data.

Algorithms developed for the competition used a wide range of time domain and frequency domain features, in addition to more complex features. Most participants developed their approaches empirically, and with machine learning approaches it is difficult to identify which features contribute predictive value to the model and which features are primarily ignored. All six algorithms used some form of spectral power in discreet frequency bands, and five of the six algorithms used time domain and/or frequency domain interchannel correlations. Both power in band and bivariate interchannel correlation have previously been shown to be independently capable of forecasting (Park *et al.*, 2011; Howbert *et al.*, 2014; Brinkmann *et al.*, 2015). While six different machine learning algorithms were used individually or as part of an ensemble in the held out data experiment, it is interesting to note that SVM was the most commonly used algorithm, appearing in four of the six participating entries. Further investigation is needed however, to assess the relative predictive value of different feature classes, and the relative capabilities of different machine learning algorithms in this context.

A large-scale online competition aimed at developing novel algorithms for seizure forecasting was successfully conducted using open access datasets from canines and humans. The kaggle.com competition format enabled direct comparison between different seizure forecasting algorithms on a common dataset, and provides a benchmark for future forecasting studies. Multiple groups using different approaches succeeded in independently developing successful algorithms for seizure forecasting, supporting the hypothesis that seizures are not random but arise from an observable preictal state. Open access to data, methods, and algorithms creates a platform for reproducible seizure forecasting research. Future studies are required to clarify what percentage of patients with epilepsy have seizures that can be forecast using iEEG, and the level of forecasting performance needed for improving outcome and quality of life.

## Acknowledgements

The authors acknowledge Cindy Nelson, Mark Bower PhD, Karla Crockett, Daniel Crepeau, and Matt Stead

MD, PhD for data collection and assistance with data processing. The canine data was recorded using devices developed by NeuroVista Inc., and we acknowledge the contributions of NeuroVista's former management and employees.

## Funding

The authors acknowledge the generous support of the American Epilepsy Society, The Epilepsy Foundation, Kaggle.com (which waived a portion of its normal fee for this competition), and the National Institutes of Health. Data collection, processing, analysis, and manuscript preparation were supported by NeuroVista Inc. and grants NIH-NINDS UH2/UH3 95495 (G.W.), U01-NS 73557 (G.W.), U24-NS063930 (B.L., G.W.), K01 ES025436-01 (J.W.), and R01-NS92882 (G.W.), the Mirowski family foundation, and Mayo Clinic.

## Supplementary material

Supplementary material is available at *Brain* online.

## References

- Aarabi A, Wallois F, Grebe R. Does spatiotemporal synchronization of EEG change prior to absence seizures? *Brain Res* 2008; 1188: 207–21.
- Adelson PD, Nemoto E, Scheuer M, Painter M, Morgan J, Yonas H. Noninvasive continuous monitoring of cerebral oxygenation pericritally using near-infrared spectroscopy: a preliminary report. *Epilepsia* 1999; 40: 1484–9.
- Andrzejak RG, Chicharro D, Elger CE, Mormann F. Seizure prediction: any better than chance? *Clin Neurophysiol* 2009; 120: 1465–78.
- Badawy R, Macdonell R, Jackson G, Berkovic S. The peri-ictal state: cortical excitability changes within 24 h of a seizure. *Brain* 2009; 132: 1013–21.
- Baumgartner C, Serles W, Leutmezer F, Pataria E, Aull S, Czech T, et al. Preictal SPECT in temporal lobe epilepsy: regional cerebral blood flow is increased prior to electroencephalography-seizure onset. *J Nucl Med* 1998; 39: 978–82.
- Berendt M, Dam M. Re: clinical presentations of naturally occurring canine seizures: similarities to human seizures. *Epilepsy Behav* 2003; 4: 198–9; author reply 9–201.
- Berendt M, Hogenhaven H, Flagstad A, Dam M. Electroencephalography in dogs with epilepsy: similarities between human and canine findings. *Acta Neurol Scand* 1999; 99: 276–83.
- Bower MR, Buckmaster PS. Changes in granule cell firing rates precede locally recorded spontaneous seizures by minutes in an animal model of temporal lobe epilepsy. *J Neurophysiol* 2008; 99: 2431–42.
- Breiman L. Bagging predictors. *Mach Learn* 1996; 24: 123–40.
- Brinkmann BH, Bower MR, Stengel KA, Worrell GA, Stead M. Large-scale electrophysiology: acquisition, compression, encryption, and storage of big data. *J Neurosci Methods* 2009; 180: 185–92.
- Brinkmann BH, Patterson EE, Vite C, Vasoli VM, Crepeau D, Stead M, et al. Forecasting seizures using intracranial EEG measures and SVM in naturally occurring canine epilepsy. *PLoS One* 2015; 10: e0133900

- Buckheit J, Donoho D. WaveLab and Reproducible Research. In: Antoniadis A, Oppenheim G, editors. *Wavelets and Statistics*. New York: Springer; 1995. p. 55–81.
- Button KS, Ioannidis JP, Mokrysz C, Nosek BA, Flint J, Robinson ES, et al. Power failure: why small sample size undermines the reliability of neuroscience. *Nat Rev Neurosci* 2013; 14: 365–76.
- Coles LD, Patterson EE, Sheffield WD, Mavoori J, Higgins J, Michael B, et al. Feasibility study of a caregiver seizure alert system in canine epilepsy. *Epilepsy Res* 2013; 106: 456–60.
- Cook MJ, O'Brien TJ, Berkovic SF, Murphy M, Morokoff A, Fabinyi G, et al. Prediction of seizure likelihood with a long-term, implanted seizure advisory system in patients with drug-resistant epilepsy: a first-in-man study. *Lancet Neurol* 2013; 12: 563–71.
- Davis KA, Sturges BK, Vite CH, Ruedebusch V, Worrell G, Gardner AB, et al. A novel implanted device to wirelessly record and analyze continuous intracranial canine EEG. *Epilepsy Res* 2011; 96: 116–22.
- Donoho DL. An invitation to reproducible computational research. *Biostatistics* 2010; 11: 385–8.
- Dowling PM. Management of canine epilepsy with phenobarbital and potassium bromide. *Can Vet J* 1994; 35: 724–5.
- Duncan JS, Smith SJ, Forster A, Shorvon SD, Trimble MR. Effects of the removal of phenytoin, carbamazepine, and valproate on the electroencephalogram. *Epilepsia* 1989; 30: 590–6.
- Farnbach GC. Serum concentrations and efficacy of phenytoin, phenobarbital, and primidone in canine epilepsy. *J Am Vet Med Assoc* 1984; 184: 1117–20.
- Feder J. *Fractals*. New York: Plenum Press; 1988.
- Fisher RS. Epilepsy from the patient's perspective: review of results of a community-based survey. *Epilepsy Behav* 2000; 1: S9–S14.
- Friedman J, Hastie T, Tibshirani R. Regularization paths for generalized linear models via coordinate descent. *J Stat Softw* 2010; 33: 1.
- Fujita S, Toyoda I, Thamattoor AK, Buckmaster PS. Preictal activity of subicular, CA1, and dentate gyrus principal neurons in the dorsal hippocampus before spontaneous seizures in a rat model of temporal lobe epilepsy. *J Neurosci* 2014; 34: 16671–87.
- Govendir M, Perkins M, Malik R. Improving seizure control in dogs with refractory epilepsy using gabapentin as an adjunctive agent. *Aust Vet J* 2005; 83: 602–8.
- Haut SR, Hall CB, LeValley AJ, Lipton RB. Can patients with epilepsy predict their seizures? *Neurology* 2007; 68: 262–6.
- Higuchi T. Approach to an irregular time series on the basis of the fractal theory. *Physica D* 1988; 31: 277–83.
- Hjorth B. EEG analysis based on time domain properties. *Electroencephalogr Clin Neurophysiol* 1970; 29: 306–10.
- Hotelling H. Analysis of a complex of statistical variables into principal components. *J Educ Psychol* 1933; 24: 417.
- Howbert JJ, Patterson EE, Stead SM, Brinkmann B, Vasoli V, Crepeau D, et al. Forecasting seizures in dogs with naturally occurring epilepsy. *PLoS One* 2014; 9: e81920.
- Ioannidis JP. Why most published research findings are false. *PLoS Med* 2005; 2: e124.
- Kiviranta AM, Laitinen-Vapaavuori O, Hielm-Bjorkman A, Jokinen T. Topiramate as an add-on antiepileptic drug in treating refractory canine idiopathic epilepsy. *J Small Anim Pract* 2013; 54: 512–20.
- Kruskal JB. Toward a practical method which helps uncover the structure of a set of multivariate observations by finding the linear transformation which optimizes a new 'index of condensation'. In: *Statistical computation*. New York: Academic Press; 1969. p. 427–40.
- Kwan P, Arzimanoglou A, Berg AT, Brodie MJ, Allen Hauser W, Mathern G, et al. Definition of drug resistant epilepsy: consensus proposal by the ad hoc task force of the ILAE commission on therapeutic strategies. *Epilepsia* 2010; 51: 1069–77.
- Kwan P, Brodie MJ. Definition of refractory epilepsy: defining the indefinable? *Lancet Neurol* 2010; 9: 27–9.
- Landis SC, Amara SG, Asadullah K, Austin CP, Blumenstein R, Bradley EW, et al. A call for transparent reporting to optimize the predictive value of preclinical research. *Nature* 2012; 490: 187–91.
- LeCun YBL, Bengio Y, Haffner P. Gradient-based learning applied to document recognition. *Proceedings of the IEEE* November 1998; 86: 2278–324.
- Leppik IE, Patterson EN, Coles LD, Craft EM, Cloyd JC. Canine status epilepticus: a translational platform for human therapeutic trials. *Epilepsia* 2011; 52 (Suppl 8): 31–4.
- Loscher W. Critical review of current animal models of seizures and epilepsy used in the discovery and development of new antiepileptic drugs. *Seizure* 2011; 20: 359–68.
- MacKay DJ. *Information theory, inference and learning algorithms*. Cambridge: Cambridge University Press; 2003.
- Marciani MG, Gotman J, Andermann F, Olivier A. Patterns of seizure activation after withdrawal of antiepileptic medication. *Neurology* 1985; 35: 1537–43.
- Mirowski P, Madhavan D, Lecun Y, Kuzniecky R. Classification of patterns of EEG synchronization for seizure prediction. *Clin Neurophysiol* 2009; 120: 1927–40.
- Mormann F, Andrzejak RG, Elger CE, Lehnertz K. Seizure prediction: the long and winding road. *Brain* 2007; 130: 314–33.
- Munana KR, Thomas WB, Inzana KD, Nettifee-Osborne JA, McLucas KJ, Olby NJ, et al. Evaluation of levetiracetam as adjunctive treatment for refractory canine epilepsy: a randomized, placebo-controlled, crossover trial. *J Vet Intern Med* 2012; 26: 341–8.
- Packer RM, Shihab NK, Torres BB, Volk HA. Clinical risk factors associated with anti-epileptic drug responsiveness in canine epilepsy. *PLoS One* 2014; 9: e106026.
- Park Y, Luo L, Parhi KK, Netoff T. Seizure prediction with spectral power of EEG using cost-sensitive support vector machines. *Epilepsia* 2011; 52: 1761–70.
- Patterson EE. Canine epilepsy: an underutilized model. *Ilar J* 2014; 55: 182–6.
- Pellegrino FC, Sica RE. Canine electroencephalographic recording technique: findings in normal and epileptic dogs. *Clin Neurophysiol* 2004; 115: 477–87.
- Petrosian A. Kolmogorov complexity of finite sequences and recognition of different preictal EEG patterns. 1995 Proceedings of the Eighth IEEE Symposium on Computer-Based Medical Systems. Lubbock, TX: IEEE; 1995. p. 212–7.
- Platt J. Probabilistic outputs for support vector machines and comparisons to regularized likelihood methods. *Adv Large Margin Classifiers* 1999; 10: 61–74.
- Potschka H, Fischer A, von Ruden EL, Hulsmeier V, Baumgartner W. Canine epilepsy as a translational model? *Epilepsia* 2013; 54: 571–9.
- Schulze-Bonhage A, Kuhn A. Unpredictability of Seizures and the Burden of Epilepsy. in *Seizure Prediction in Epilepsy: From Basic Mechanisms to Clinical Applications* Wiley VCH: Verlag GmbH & Co. KGaA, Weinheim 2008. pp. 1–10.
- Snyder DE, Echaz J, Grimes DB, Litt B. The statistics of a practical seizure warning system. *J Neural Eng* 2008; 5: 392–401.
- Stacey W, Le Van Quyen M, Mormann F, Schulze-Bonhage A. What is the present-day EEG evidence for a preictal state? *Epilepsy Res* 2011; 97: 243–51.
- Teixeira CA, Direito B, Bandarabadi M, Le Van Quyen M, Valderrama M, Schelter B, et al. Epileptic seizure predictors based on computational intelligence techniques: a comparative study with 278 patients. *Comput Methods Programs Biomed* 2014; 114: 324–36.
- Vapnik VN, Vapnik V. *Statistical learning theory*. New York: Wiley; 1998.